Inorg. Chem. **2002**, *41*, 790–795

o-Iminobenzosemiquinonato Complexes of Mn(III) and Mn(IV). Synthesis and Characterization of $[Mn^{III}(L^{ISQ})_2(L^{AP})]$ ($S_t = 1$) and $[Mn^{IV}(L^{ISQ})_2(L^{AP}\text{-}H)]$ ($S_t = {}^1/_2$)

Hyungphil Chun, Phalguni Chaudhuri, Thomas Weyhermüller, and Karl Wieghardt*

Max-Planck-Institut für Strahlenchemie, Stiftstrasse 34-36, D-45470 Mülheim an der Ruhr, Germany

Received August 7, 2001

From the reaction of $[Mn^{III}_3(\mu\text{-}O)(\mu\text{-}CH_3CO_2)_6]CH_3CO_2$ (manganese(III) acetate) and 2-anilino-4,6-di-*tert*-butylphenol (1:3) in methanol under anaerobic conditions, dark brown-black crystals of $[Mn^{III}(L^{ISQ})_2(L^{AP})]$ (**1**) were obtained in ~30% yield. $(L^{AP})^-$ represents the closed-shell *o*-aminophenolate(–) form of the above ligand, and $(L^{ISQ})^-$ is the monoanionic π radical form *o*-iminobenzosemiquinonate(–) ($S_{rad} = {}^1/_2$). Complex **1** can be deprotonated at the $(L^{AP})^-$ ligand and one-electron-oxidized by air, yielding crystals of $[Mn^{IV}(L^{ISQ})_2(L^{AP}\text{-}H)]$ (**2**), where $(L^{AP}\text{-}H)^{2-}$ represents the closed-shell, dianionic *o*-amidophenolate(2–) form of the above ligand. The structures of **1** and **2** have been determined by X-ray crystallography at 100 K. The protonation and oxidation levels of the ligands and of the metal ions have been unequivocally established: both complexes contain two π radical ligands, **1** contains a Mn^{III} ion, and **2** contains a Mn^{IV} ion. The spins of the radicals ($S_{rad} = {}^1/_2$) couple strongly antiferromagnetically with the d^4 and d^3 configuration of the Mn ions in **1** and **2**, respectively, yielding the observed ground states of $S = 1$ for **1** and $S = {}^1/_2$ for **2**. This has been established by temperature-dependent susceptibility measurements (2–300 K) and S- and X-band EPR spectroscopy.

Introduction

In a series of papers[1−4] we have recently shown that *O,N*-coordinated *o*-aminophenolate ligands are redox noninnocent in the sense that in a given complex they can be bound to a transition metal ion as *o*-aminophenolate(−), $(L^{AP})^-$, as *o*-amidophenolate(2−), $(L^{AP}\text{-}H)^{2-}$, or as *o*-iminobenzosemiquinonate(−) π radical, $(L^{ISQ})^-$. We have shown that it is possible to unambiguously discern these forms in a complex by high-quality X-ray crystallography if the estimated experimental error of the C−C, C−O, and C−N bond lengths is not larger than ±0.015 Å (3σ). Chart 1 shows the geometric features observed for (i) $(L^{AP})^-$ containing an aromatic aminophenol ring with six equivalent C−C bonds, a long C−N bond at 1.47 Å, and a relatively long C−O bond at 1.35 Å, (ii) $(L^{AP}\text{-}H)^{2-}$, where only the shorter C−N bond at 1.38 Å differs significantly from those of $(L^{AP})^-$, and (iii) $(L^{ISQ})^-$, where the six-membered ring displays a quinoid-type distortion comprising a short, a long, and another short C−C bond followed by three long ones and,

Chart 1. Geometrical Features of the Ligands

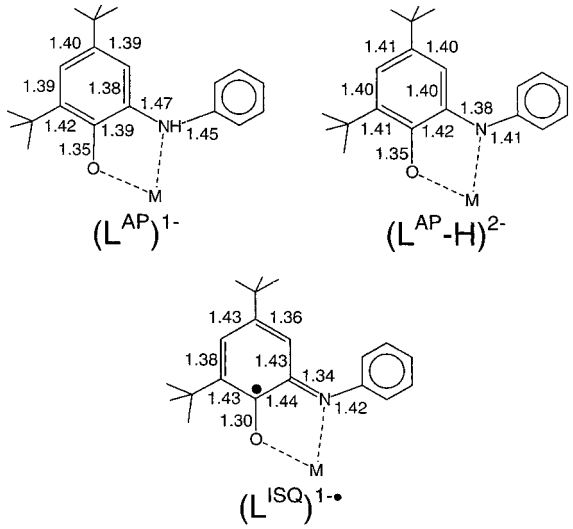

* Author to whom correspondence should be addressed. E-mail: wieghardt@mpi-muelheim.mpg.de.

(1) Verani, C. N.; Gallert, S.; Bill, E.; Weyhermüller, T.; Wieghardt, K.; Chaudhuri, P. *Chem. Commun.* **1999**, 1747.
(2) Chaudhuri, P.; Verani, C. N.; Bill, E.; Bothe, E.; Weyhermüller, T.; Wieghardt, K. *J. Am. Chem. Soc.* **2001**, *123*, 2213.
(3) Chun, H.; Verani, C. N.; Chaudhuri, P.; Bothe, E.; Bill, E.; Weyhermüller, T.; Wieghardt, K. *Inorg. Chem.* **2001**, *40*, 4157.
(4) Chun, H.; Weyhermüller, T.; Bill, E.; Wieghardt, K. *Angew. Chem., Int. Ed.* **2001**, *40*, 2489.

10.1021/ic010860w CCC: $22.00
Published on Web 01/23/2002

in addition, both the C−O and C−N distances are significantly shorter (1.30 and 1.34 Å, respectively) than those in $(L^{AP})^-$ and $(L^{AP}\text{-}H)^{2-}$.

Thus, we have previously structurally characterized the following pseudooctahedral first-row transition-metal ion complexes:[3] $[Cr^{III}(L^{ISQ})_3]$, $[Fe^{III}(L^{ISQ})_3]$, and $[Co^{III}(L^{ISQ})_3]$,[1] all of which contain three equivalent *O*,*N*-coordinated *o*-iminosemiquinonato(−) π radicals ($S_{rad} = {}^1/_2$). It was shown that the spins of these ligand radicals couple intramolecularly to the electron spins of a half-filled t_{2g} subshell of the metal ion, yielding a ground state of $S_t = 0$ for the chromium(III) and $S_t = 1$ for the high-spin ferric complex. In $[Co^{III}(L^{ISQ})_3]$ containing a low-spin cobalt(III) ion with a filled t_{2g} subshell, the radical spins couple weakly ferromagnetically, $S_t = {}^3/_2$. The most intriguing charge distribution was found in some vanadium complexes. Thus, two octahedral species were structurally characterized, namely, $[V^V(L^{ISQ})(L^{AP}\text{-}H)_2]$ ($S_t = {}^1/_2$) and $[V^V(L^{AP}\text{-}H)_2(L^{AP})]$ ($S_t = 0$). Surprisingly, $[V^{III}(L^{ISQ})_3]$ does not exist.

Here we report the synthesis and molecular and electronic structures of two related complexes containing a central manganese ion: $[Mn^{III}(L^{ISQ})_2(L^{AP})]$ ($S_t = 1$) (**1**) and $[Mn^{IV}(L^{ISQ})_2(L^{AP}\text{-}H)]$ ($S_t = {}^1/_2$) (**2**). The ligand used in this investigation is 2-anilino-4,6-di-*tert*-butylphenol. We will compare the present results with those reported by Attia and Pierpont[5] for the compound $[Mn^{IV}(3,6\text{-}DBSQ)_2(3,6\text{-}DBCat)]$.

Experimental Section

The ligand 2-anilino-4,6-di-*tert*-butylphenol, $H[L^{AP}]$, was prepared according to published procedures.[2]

$[Mn^{III}(L^{ISQ})_2(L^{AP})]$ (1). Under an argon blanketing atmosphere the ligand $H[L^{AP}]$ (0.49 g, 1.6 mmol) was dissolved in methanol (20 mL). To this solution were added a solution of $Li(OC_2H_5)$ in ethanol (1.0 M, 3.5 mL) and solid manganese(III) acetate (0.14 g). The dark red solution was heated to reflux for 1 h under argon. Slow evaporation of the solvent at 20 °C under argon initiated the precipitation of dark, brown-black crystals of **1**. Yield: 0.15 g (30%). A single crystal from the raw product was used for the X-ray structure determination. Anal. Calcd for $C_{60}H_{76}N_3O_3Mn$ (942.2 g mol^{-1}): C, 76.49; H, 8.13; N, 4.46. Found: C, 76.5; H, 8.0; N, 4.6. ESI-MS (CH_2Cl_2, positive ion): $m/z = 941$ $\{M\}^+$. UV−vis (CH_2Cl_2, 20 °C): 197 nm ($\epsilon = 1.5 \times 10^5$ L mol^{-1} cm^{-1}), 285 (3.4×10^4), 437 (1.1×10^4), 474 (1.2×10^4), 775 (5.9×10^3).

$[Mn^{IV}(L^{ISQ})_2(L^{AP}\text{-}H)]$ (2). The ligand $H[L^{AP}]$ (0.54 g, 1.8 mmol) and $Na[OC_2H_5]$ (0.50 g, 7.4 mmol) were dissolved in absolute ethanol (45 mL) in the presence of air at 20 °C. To the deep red solution was added a solution of manganese(III) acetate (0.15 g) in ethanol (45 mL). After the solution was stirred at 20 °C for 1 h under argon, the solvent was allowed to slowly evaporate by passing an argon stream through the solution, whereupon a small amount of dark crystals of **2** precipitated. Yield: 0.14 g (27%). A single crystal selected from the raw product was used for the X-ray structure determination. Anal. Calcd for $C_{60}H_{75}N_3O_3$ (941.2 g mol^{-1}): C, 76.57; H, 8.03; N, 4.46. Found: C, 76.6; H, 8.0; N, 4.4. EI-MS: $m/z = 940$ $\{M\}^+$, 645 $\{M - L\}^+$. UV−vis (CH_2Cl_2, 20 °C): 195 nm ($\epsilon = 1.4 \times 10^5$ L mol^{-1} cm^{-1}), 287 (2.9×10^4), 437 (1.0×10^4), 474 (1.2×10^4), 776 (5.9×10^3).

Physical Measurements. The electronic spectra of the complexes were recorded on an HP 8452A diode array spectrophotometer (range 221−1100 nm) and on a Perkin-Elmer Lambda 9 spectrophotometer (range 220−2500 nm). Temperature-dependent (2−298 K) magnetization data were recorded on a SQUID magnetometer (MPMS Quantum design) in an external magnetic field of 1.0 T. The experimental susceptibility data were corrected for underlying diamagnetism by the use of tabulated Pascal's constants. EPR spectra were recorded on a Bruker ESP 300 spectrometer. The spectra were simulated by iteration of the (an)isotropic *g* values, hyperfine coupling constants, and line widths. We thank Dr. F. Neese for a copy of his EPR simulation program.

Table 1. Crystallographic Data for $[Mn(L^{ISQ})_2(L^{AP})]$ (**1**) and $[Mn(L^{ISQ})_2(L^{AP}\text{-}H)]$ (**2**)

	1	**2**
empirical formula	$C_{60}H_{76}MnN_3O_3$	$C_{60}H_{75}MnN_3O_3$
fw	942.18	941.17
space group	$P2_12_12_1$ (no. 19)	$P\bar{1}$ (no. 2)
a, Å	12.9544(8)	10.4837(8)
b, Å	17.5606(12)	14.7941(10)
c, Å	23.183(2)	17.8002(12)
α, deg	90	97.79(1)
β, deg	90	93.77(1)
γ, deg	90	95.53(1)
V, Å	5273.9(7)	2713.8(3)
Z	4	2
T, K	100(2)	100(2)
ρ_{calcd}, g cm^{-3}	1.187	1.152
μ(Mo Kα), cm^{-1}	2.97	2.88
diffractometer	Nonius Kappa-CCD	Nonius Kappa-CCD
no. of reflns collected	36115	23443
no. of unique reflns/[$I > 2\sigma(I)$]	9260/7573	12333/9338
no. of params	625	604
θ range, deg	1.45−25.00	3.84−27.50
R1[a] [$I > 2\sigma(I)$]	0.0474	0.0502
wR2[b] [$I > 2\sigma(I)$]	0.0959	0.1026
GOF[c]	1.040	1.027
absolute structure param	0.03(2)	
residual density, e Å^{-3}	+0.25/0.30	+0.44/0.31

[a] $R1 = \sum||F_o| - |F_c||/\sum|F_o|$. [b] $wR2 = [\sum[w(F_o^2 - F_c^2)^2]/\sum[w(F_o^2)^2]]^{1/2}$, where $w = 1/\sigma^2(F_o^2) + (aP)^2 + bP$, $P = (F_o^2 + 2F_c^2)/3$. [c] $GOF = [\sum[w(F_o^2 - F_c^2)^2]/(n - p)]^{1/2}$, where n = number of reflections and p = number of refined parameters.

X-ray Crystallographic Data Collection and Refinement of the Structures. Brown-black single crystals of **1** and **2** were coated with perfluoropolyether, picked up with glass fibers, and mounted on a Nonius Kappa-CCD diffractometer equipped with a rotating Mo anode setup and a nitrogen cold stream operating at 100 K. Graphite-monochromated Mo Kα radiation ($\lambda = 0.71073$ Å) was used. The crystallographic data of the compounds are listed in Table 1. The cell constants were obtained from a least-squares fit of the diffraction angles of several thousand strong reflections. The intensity data were corrected for Lorentz and polarization effects. The crystal faces of $[Mn^{III}(L^{ISQ})_2(L^{AP})]$ were determined, and the face-indexed correction routine embedded in ShelXTL[6] was used to account for absorption, giving minimum and maximum transmission factors of 0.869 and 0.945, while the intensity data of $[Mn^{IV}(L^{ISQ})_2(L^{AP}\text{-}H)]$ were left uncorrected. The Siemens ShelXTL[1] software package was used for the solution, refinement, and artwork of the structures, and neutral atom scattering factors of the program were used. Non-hydrogen atoms were refined anisotropically, and hydrogen atoms were placed at calculated positions and refined as riding atoms with isotropic displacement parameters. The hydrogen atom at N(1) in $[Mn^{III}(L^{ISQ})_2(L^{AP})]$ was easily located from the difference map and refined with only its isotropic temperature factor restricted to 1.2 times the factor of N(1).

(5) Attia, A. S.; Pierpont, C. G. *Inorg. Chem.* **1998**, *37*, 3051.

(6) ShelXTL V.5, Siemens Analytical X-ray Instruments, Inc., 1994.

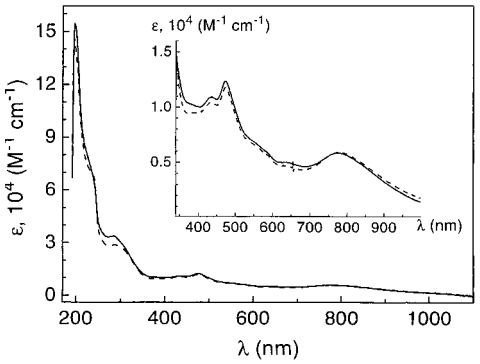

Figure 1. Electronic spectra of **1** (solid line) and **2** (broken line) in ethanol under an Ar atmosphere.

Results

Synthesis. When a reaction mixture of the ligand H[L^{AP}], Li(OC_2H_5), and manganese(III) acetate, [Mn^{III}_3(μ_3-O)(CH_3CO_2)$_6$]CH_3CO_2, in methanol was heated to reflux under an argon atmosphere, a dark red solution was obtained. Upon slow evaporation of the solvent under argon, dark brown-black crystals of [Mn^{III}(L^{ISQ})$_2$(L^{AP})] (**1**) precipitated in ~30% yield based on the total amount of manganese ions present. Since the reaction was carried out in the absence of an external oxidant (dioxygen), the above yield is in good agreement with the stoichiometry depicted in eq 1.

$$3Mn^{III} + 3H[L^{AP}] \rightarrow [Mn^{III}(L^{ISQ})_2(L^{AP})] + 2Mn^{II} \quad (1)$$

When the same reaction as described above was carried out in the presence of air, dark crystals of [Mn^{IV}(L^{ISQ})$_2$(L^{AP}-H)] (**2**) were obtained.

In the infrared, complex **1** exhibits a weak ν(N−H) stretching frequency at 3324 cm^{-1}, which is absent in the IR spectrum of **2**.

Single crystals suitable for X-ray analysis of **1** and **2** were selected from the crude materials obtained from the above reactions. We have not found suitable conditions for successful recrystallizations. We note that if dioxygen is not rigorously excluded in preparations of **1** or if triethylamine is used instead of lithium/sodium ethoxide as base, mixtures of **1** and **2** are inevitably obtained. Also, the amount of base used must be 2 equiv or slightly less per ligand for **1** and an excess for **2** to avoid the formation of analytically indistinguishable mixtures of **1** and **2**. This was established from magnetic susceptibility measurements (see below). Pure samples of **1** display an effective magnetic moment of 2.8 μ_B at 298 K, whereas **2** has a μ_{eff}(298 K) of 2.0 μ_B, and impure samples of **1** exhibit apparent values of μ_{eff} ranging from 2.2 to 2.4 μ_B.

Compound **1** is very oxygen-sensitive. A dark brown solution of **1** in CH_2Cl_2 changes color to red immediately after being exposed to air. Such a solution exhibits the same EPR spectrum as a genuine solution of **2**.

Interestingly, the electronic spectra of **1** and **2** in ethanol solution measured under strictly anaerobic conditions are very similar. Figure 1 shows the spectra in the range 200−1100 nm. The intense transitions at 437, 474, and 775 nm are assigned to intraligand $\pi-\pi^*$ transitions of the (L^{ISQ})$^-$ ligands. They resemble closely those reported for [(dmtacn)-Cu^{II}(L^{ISQ})]$^+$, where dmtacn represents 1,4-dimethyl-triazacyclononane.[2] Both complexes **1** and **2** do not exhibit further transitions in the range 1000−2500 nm, and the intensity of the transitions in the visible is temperature-independent (10−300 K).

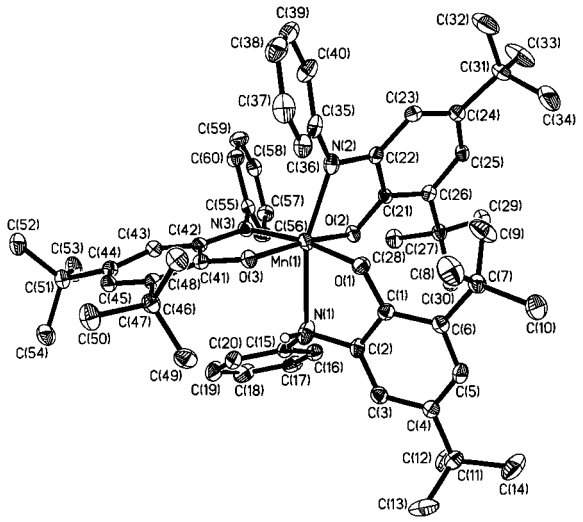

Figure 2. Perspective view of the neutral molecule in **1** (the small open circle at N1 represents a hydrogen atom).

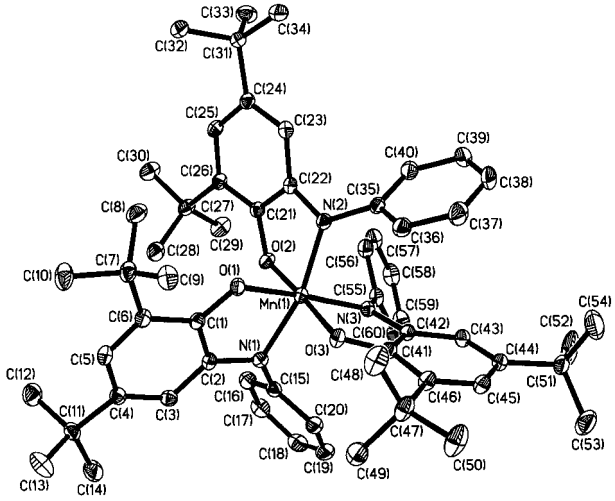

Figure 3. Perspective view of the neutral molecule in **2**.

The spectra of **1** and **2** in the visible are thus dominated by the two (L^{ISQ})$^-$ ligands present in both compounds.

Crystal Structures. The crystal structures of complexes **1** and **2** have been determined by single-crystal X-ray crystallography at 100(2) K. Figure 2 shows the structure of a neutral molecule in crystals of **1**, and Figure 3 that of **2**. Selected metal-to-oxygen and metal-to-nitrogen bond lengths are summarized in Table 2. The geometrical features of the *O*,*N*-coordinated ligands in both structures are within an experimental error of ±0.015 Å identical to those shown in Chart 1.

Complexes [Cr^{III}(L^{ISQ})$_3$], [Fe^{III}(L^{ISQ})$_3$], [V^V(L^{AP}-H)$_2$(L^{ISQ})], and **1** crystallize in the orthorhombic chiral space group $P2_12_12_1$ with four molecules per unit cell.[1,2] The neutral molecules possess C_1 symmetry and exist in two enantio-

Table 2. Selected Bond Distances (Å)

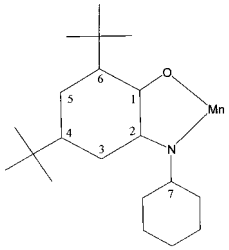

	1		2	
Mn−O1	1.896(2)		1.904(1)	
Mn−O2	1.899(2)		1.873(1)	
Mn−O3	1.932(2)		1.913(1)	
Mn−N1	2.345(3)		1.996(2)	
Mn−N2	2.082(3)		1.963(2)	
Mn−N3	1.950(2)		1.957(2)	
		$(L^{ISQ})^-$		
C1−O	1.303(3)	1.309(3)	1.305(2)	1.296(2)
C2−N	1.354(4)	1.350(4)	1.348(2)	1.358(2)
C7−N	1.414(4)	1.421(4)	1.418(2)	1.425(2)
C1−C2	1.441(4)	1.413(4)	1.436(3)	1.434(2)
C2−C3	1.404(4)	1.420(4)	1.426(3)	1.426(3)
C3−C4	1.364(4)	1.354(4)	1.361(3)	1.364(3)
C4−C5	1.421(4)	1.423(4)	1.438(3)	1.435(3)
C5−C6	1.377(4)	1.379(4)	1.376(3)	1.369(3)
C6−C1	1.426(4)	1.430(4)	1.426(3)	1.424(3)
		$(L^{AP})^-$ or $(L^{AP}\text{-H})^{2-}$		
C1−O	1.339(4)		1.342(2)	
C2−N	1.422(4)		1.395(2)	
C7−N	1.396(4)		1.412(2)	
C1−C2	1.399(4)		1.412(3)	
C2−C3	1.383(4)		1.402(3)	
C3−C4	1.382(4)		1.383(3)	
C4−C5	1.387(5)		1.412(3)	
C5−C6	1.388(4)		1.389(3)	
C6−C1	1.409(4)		1.411(3)	

meric forms. They crystallize with spontaneous resolution. The C_3 symmetric diastereomer of any of the above compounds has not been observed.

$[Co^{III}(L^{ISQ})_3]$ crystallizes in the monoclinic space group $P2_1/n$ ($Z = 4$) and **2** in the triclinic space group $P\bar{1}$ ($Z = 2$). Again, only the C_1 symmetric diastereomer has been isolated, but both enantiomeric forms are present in the unit cell. These observations corroborate the notion that it is misleading to infer from the fact that the complexes $[M(3,5\text{-}SQ)_3]$ (M = V, Cr, Fe)[7,8] are isomorphous that the molecules are also isostructural and, in particular, that they contain the same charge distributions among the different metal ions and ligands, i.e., three *o*-semiquinonato(−) radicals and a trivalent metal ion.

The neutral molecule in crystals of **1** contains two *O*,*N*-coordinated *o*-iminobenzosemiquinonate(−) π radical ligands, $(L^{ISQ})^-$, as is clearly borne out by the observation that (i) both nitrogens are sp^2 hybridized and not protonated, (ii) the six-membered ring of the iminobenzosemiquinonate part displays the typical quinoid distortions, and (iii) the C−O and C−N bond lengths are short, approaching double bonds. In contrast, the third ligand in **1** is protonated at the amine group; the nitrogen is sp^3 hybridized, and the C−O and C−N bond lengths at 1.34 and 1.42 Å (±0.015 Å), respectively, are long and typical for phenolates and aromatic amines, respectively. In addition, the C−C bonds of the aminophenol part are equidistant at 1.39 ± 0.015 Å. These data unambiguously define the oxidation and protonation levels of the three ligands in **1** as two $(L^{ISQ})^-$ ligands and one $(L^{AP})^-$ ligand, which renders the central metal ion a Mn(III) (d^4) ion. This is nicely corroborated by the observed Mn−O and Mn−N bond distances: the N1−Mn−N2 axis defines an elongated Jahn−Teller axis of a high-spin d^4 ion in a distorted octahedral ligand field. In summary, the crystal structure of **1** unequivocally indicates a charge distribution of $[Mn^{III}(L^{ISQ})_2(L^{AP})]$.

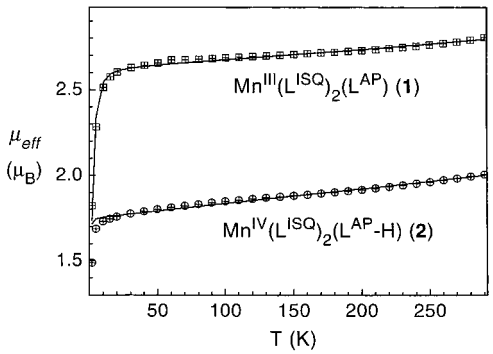

Figure 4. Temperature dependence of the magnetic moments of **1** and **2**. The solid lines represent the best fits using the parameters given in the text.

The neutral molecule in crystals of **2** also contains two *O*,*N*-coordinated $(L^{ISQ})^-$ radicals which exhibit within experimental error the same structural features as those in **1**. In contrast to **1**, the third ligand is *N*-deprotonated; the corresponding nitrogen is sp^2 hybridized (the sum of the three bond angles C22−N2−Mn, C35−N2−Mn, and C22−N2−C35 is 355.5°). The six C−C bonds of the amidophenolate ring are equidistant at 1.40 ± 0.015 Å, and the C−O and C−N distances at 1.34 ± 0.015 and 1.40 ± 0.015 Å are long. This ligand displays the characteristic features of an *O*,*N*-coordinated aromatic dianion, $(L^{AP}\text{-H})^{2-}$ (Chart 1). If this assignment is correct, the central Mn ion must be ascribed a +4 (d^3) oxidation level. The observed Mn−O and Mn−N bond distances in **2** support this view; they are shorter than the corresponding bonds in **1**, and the pseudooctahedral O_3N_3Mn polyhedron does not show the Jahn−Teller distortion described above for **1**. The average Mn−O/N distance in **1** is 2.017 Å, whereas in **2** this distance is 1.934 Å. The difference of 0.083 Å is quite close to the difference of the ionic radii calculated for an octahedrally coordinated high-spin Mn^{III} ion and a Mn^{IV} ion: 0.115 Å = 0.785 −0.67 Å. The crystal structure of **2** is in excellent agreement with a charge distribution of $[Mn^{IV}(L^{ISQ})_2(L^{AP}\text{-H})]$.

Magnetic Susceptibility Data and EPR Spectra. The electronic ground states of complexes **1** and **2** have been established from variable-temperature (2−300 K) magnetic susceptibility measurements by using a SQUID magnetometer in an external magnetic field of 1.0 T.

Figure 4 shows the temperature dependence of the magnetic moment, μ_{eff}, for **1** and **2**. On lowering the

(7) Cass, M. E.; Greene, D. L.; Buchanan, R. M.; Pierpont, C. G. *J. Am. Chem. Soc.* **1983**, *105*, 2680.
(8) Cass, M. E.; Gordon, N. R.; Pierpont, C. G. *Inorg. Chem.* **1986**, *25*, 3962.

temperature, μ_{eff} of **1** decreases monotonically from 2.8 μ_B at 300 K to 2.65 μ_B at 30 K and, similarly, μ_{eff} of **2** decreases from 2.0 μ_B at 300 K to 1.7 μ_B at 20 K. This behavior indicates an $S = 1$ ground state for **1** and $S = {}^1/_2$ for **2**. Two exchange coupling constants have been considered in the simulations shown as solid lines in Figure 4 based on the Hamiltonian, eq 2.

$$H = -2J(S_1S_2 + S_2S_3) - 2J_{13}(S_1S_3) + \sum \mu_B g_i S_i B_i \quad (2)$$

Here the coupling constant J corresponds to the coupling between a ligand radical ($S = {}^1/_2$) and the adjacent metal ion ($S_{Mn} = 2$ in **1** and ${}^3/_2$ in **2**) and J_{13} represents the coupling between two remote ligand radicals. Since J and J_{13} are strongly correlated, numerical solutions obtained do not represent—a priori—unique solutions with a physical meaning. The intramolecular coupling between the ligand radicals in octahedral $[Co^{III}(L^{ISQ})_3]$ containing a low-spin Co^{III} ion ($S_{Co} = 0$, d^6) has been established to be weakly ferromagnetic ($J_{13} = 59$ cm^{-1}, $J_{12} = J_{23} = 9$ cm^{-1}).[1] For $Cr^{III}(L^{ISQ})_3$ and $Fe^{III}(L^{ISQ})_3$, however, it has not been possible nor physically meaningful to derive information on the intraligand coupling because the overall magnetic behavior is dominated by much stronger antiferromagnetic interactions between ligand radicals and metal-based unpaired d-electrons.[3] The same holds true for compounds **1** and **2**, where the decrease of μ_{eff} on lowering the temperature could well be fitted by a single coupling constant J and temperature-independent paramagnetism (TIP), with J_{13} set to 0. Setting J_{13} to any number greater than 0 and/or allowing it to vary during the fitting procedures did not make a significant difference in the final results, which gave the J large negative values. Therefore, we have chosen to fix the exchange coupling constant $J_{13} = 0$ in the fitting procedures for **1** and **2**. The data for **1** and **2** were satisfactorily fitted using a single coupling constant J which by and large should correspond to coupling between the radical and a Mn ion. Satisfactory fits for **1** were obtained using the following parameters: $S_1 = S_3 = {}^1/_2$, $S_2 = 2.0$, $g = 2.0$ (fixed), $J_{13} = 0$ (fixed), $J = -300$ cm^{-1}, $|D_{S=1}| = 3.4$ cm^{-1}, $\chi_{TIP} = 4 \times 10^{-4}$ cm^3 mol^{-1}, a paramagnetic impurity of **2** of 20%. For **2** the following parameters were obtained: $S_1 = S_3 = {}^1/_2$, $S_2 = {}^3/_2$, $g = 2.01$ (fixed), $J_{13} = 0$ (fixed), $J = -470$ cm^{-1}, $\chi_{TIP} = 4 \times 10^{-4}$ cm^3 mol^{-1}. The g value was fixed to 2.01 in accordance with the low-temperature X-band EPR experiment (see below). Hence, a strong antiferromagnetic coupling between the ligand radicals and the Mn ions is established for both complexes.

The metal-based $S = {}^1/_2$ ground state of **2** has also been established by S- and X-band EPR spectroscopy. Figure 5 shows the spectra of **2** in CH_2Cl_2 solution at 298 and 10 K for the X-band and at 25 K for the S-band and the corresponding simulations. The spectrum at 298 K displays an isotropic signal at $g_{iso} = 1.983$ with hyperfine coupling to the $I = {}^5/_2$ ^{55}Mn nucleus of $A_{iso} = 99 \times 10^{-4}$ cm^{-1}, and in addition, superhyperfine coupling to three ^{14}N donor atoms ($I = 1$) is clearly detected, $A(^{14}N) = 4 \times 10^{-4}$ cm^{-1}. In frozen solution at 10 K a rhombic signal is observed: $g_1 = 1.998$, $g_2 = 2.005$, $g_3 = 2.020$ ($g_{iso} = 2.0104$), $A_1(^{55}Mn) = 116 \times 10^{-4}$ cm^{-1}, $A_2(^{55}Mn) = 76 \times 10^{-4}$ cm^{-1}, $A_3(^{55}Mn) = 98 \times 10^{-4}$ cm^{-1} ($A_{iso}(^{55}Mn) = 97 \times 10^{-4}$ cm^{-1}). From the S-band spectrum the following parameters were obtained: $g_1 = 2.021$, $g_2 = 2.048$, $g_3 = 2.064$, $A_1(^{55}Mn) = 128 \times 10^{-4}$ cm^{-1}, $A_2(^{55}Mn) = 101 \times 10^{-4}$ cm^{-1}, $A_3(^{55}Mn) = 69 \times 10^{-4}$ cm^{-1}, $A_{iso}(^{55}Mn) = 99 \times 10^{-4}$ cm^{-1}. These spectra resemble closely that reported for $[Mn^{IV}(Cat\text{-}N\text{-}SQ)_2]$.[10]

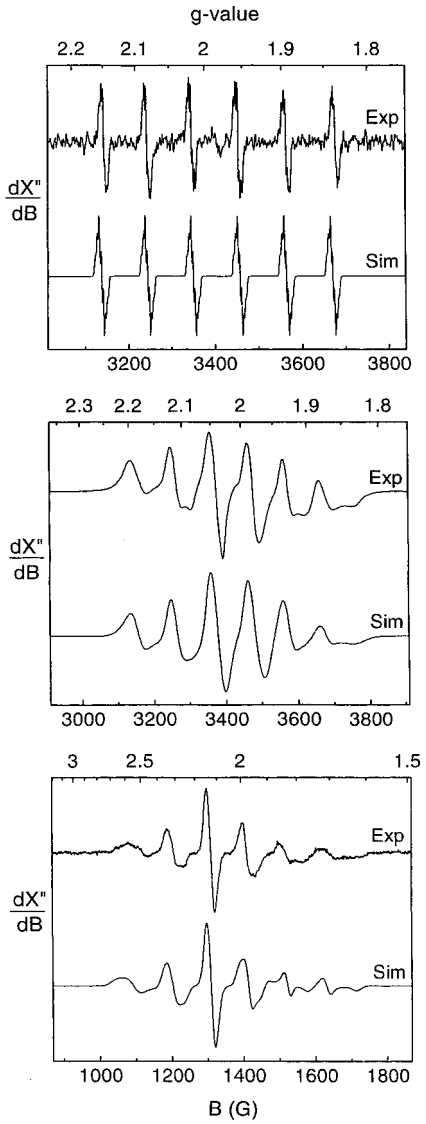

Figure 5. EPR spectra of **2** in CH_2Cl_2 solution. Bottom: S-band at 25 K (conditions: frequency 3.905 GHz; power 0.21 mW; modulation amplitude 6 G). Middle: X-band at 10 K (conditions: frequency 9.644 GHz; power 0.10 mW; modulation amplitude 10 G). Top: X-band at 298 K (conditions: frequency 9.451 GHz; power 10 mW; modulation amplitude 2G).

Discussion

In 1998 Attia and Pierpont[5] reported the synthesis and structural characterization of $[Mn^{IV}(3,6\text{-}DBSQ)_2(3,6\text{-}DBCat)]$, where 3,6-DBSQ represents the *O*,*O*-coordinated monoanionic π radical 3,6-di-*tert*-butylsemiquinonate(−) and 3,6-DBCat is the *O*,*O*-coordinated, closed-shell dianion 3,6-

(9) Cooper, S. R.; Koh, Y. G.; Raymond, K. N. *J. Am. Chem. Soc.* **1982**, *104*, 4, 5092.
(10) Swarnabala, G.; Rajasekharan, M. V.; Padhye, S. *Chem. Phys. Lett.* **1997**, *267*, 539.

di-*tert*-butylcatecholate(2−). This neutral complex has an $S = {}^1/_2$ ground state; its magnetic moment has been reported to be 1.67 μ_B at 5 K but 3.71 μ_B at 305 K. Its anisotropic EPR spectrum at 77 K ($CHCl_3$ glass) yields $g_{||} = 1.998$, $g_\perp = 2.048$, $A_{||}(^{55}Mn) = 137 \times 10^{-4}$ cm^{-1}, and $A_\perp(^{55}Mn) = 80 \times 10^{-4}$ cm^{-1}. These data are in excellent agreement with those reported here for **2** for which a charge distribution of $[Mn^{IV}(L^{ISQ})_2(L^{AP}\text{-}H)]$ has been established.

A significant and very interesting difference between the two complexes with respect to their electronic structures exists. $[Mn^{IV}(3,6\text{-}DBSQ)_2(3,6\text{-}DBCat)]$ has been shown to exhibit a broad, temperature-dependent charge-transfer band at 2300 nm, the intensity of which increases with decreasing temperature. This behavior has been interpreted in terms of valence tautomerism in the solid state between the redox isomers $[Mn^{IV}(3,6\text{-}DBSQ)_2(3,6\text{-}DBCat)]$ and $[Mn^{III}(3,6\text{-}DBSQ)_3]$. In contrast, **2** does not display this temperature-dependent redistribution of charge (no transition between 1100 and 2500 nm has been observed). The oxidation levels of the ligands as two $(L^{ISQ})^-$ ligands and one $(L^{AP}\text{-}H)^{2-}$ ligand and the Mn^{IV} ion in **2** remain fully localized in the solid state in the temperature range 2−300 K. The antiferromagnetic coupling between the radical ligands and the Mn^{IV} ion is significantly stronger in **2** than in Attia and Pierpont's complex. We ascribe this effect to a significantly larger covalency of the Mn−N bonds in **2** as compared with the corresponding Mn−O bonds in the bis(semiquinonato) complex.

Acknowledgment. We thank the Fonds der Chemischen Industrie for financial support. H.C. is grateful to the Alexander von Humboldt Foundation for a fellowship. We thank Dr. C. N. Verani for the initial experiments.

Supporting Information Available: Complete listings of crystallographic details, atom coordinates, bond lengths and bond angles, thermal displacement parameters, and calculated positional parameters for complexes **1** and **2**. This material is available free of charge via the Internet at http://pubs.acs.org.

IC010860W